NdS_2 formation in Nd-doped pyrite films

1997 J. Phys.: Condens. Matter 9 9483

(http://iopscience.iop.org/0953-8984/9/44/005)

J. Phys.: Condens. Matter **9** (1997) 9483–9495. Printed in the UK PII: S0953-8984(97)84256-7

NdS_2 formation in Nd-doped pyrite films

C de las Heras and L E Bausá

Departamento de Fisica de Materiales C-IV and Instituto Nicolás Cabrera, Facultad de Ciencias, Universidad Autónoma de Madrid, Cantoblanco, 28049 Madrid, Spain

Received 13 May 1997, in final form 4 July 1997

Abstract. Nd-doped iron pyrite thin films have been obtained for the first time by flash evaporation of natural pyrite with Nd_2O_3 powder on glass substrates. Thermal treatments in a sulphur atmosphere were performed at different temperatures in order to improve the crystal quality of the films. The effects of annealing temperature on the structural, electrical and optical properties of the Nd-doped films have been studied and compared to those of undoped pyrite films prepared and treated by the same methods. Thermal treatment induces changes in the Nd stage in the films which affect the structural and electrical parameters. The presence of a segregated NdS_2 phase is observed for high annealing temperature due to Nd diffusion in the pyrite lattice.

1. Introduction

The preparation and characterization of rare-earth-ion-doped materials in thin-film form is now an active field of research [1–4]. The aim of these works is to benefit from the optical properties of the rare earth ion emission to be incorporated in miniaturized devices.

In particular, Nd^{3+} ions are the most widely used activators in solid state lasers and stimulated emission has been obtained for a great number of host matrices [5].

On the other hand, the association of semiconductor materials and the optical properties of rare earth ions is particularly interesting in view of a new generation of optoelectronic devices. A number of works have been recently devoted to the study of preparation and characterization of rare-earth-ion-doped semiconductor thin films, and the luminescence of rare earth ions in semiconductor thin films has been studied by some authors [6–11].

Pyrite thin films are easily obtained by a variety of techniques and they have been successfully doped with different elements [12] in order to modify their electrical properties, but to date luminescence from pyrite films has not been reported. However, similar compounds have been successfully doped with rare earth ions and their luminescent properties have been studied [13].

Nd-doped iron pyrite films have been obtained for the first time in this work. The aim of this paper is to study the preparation method and the structural properties of the obtained films, as a first step to investigate the luminescence properties of these films. A preliminary optical study is performed.

In this work, a detailed study of the changes in the pyrite structure induced by the presence of Nd ions is carried out, and a series of thermal treatments has been used in order to modify the incorporation or aggregation stage of Nd inside the pyrite host. X-ray diffraction diagrams are used to determine the variation of the lattice parameter, S/Fe

0953-8984/97/449483+13$19.50

relation, crystalline size and microstrain distribution and the obtained results are compared with those of undoped pyrite films. The influence of Nd ions on electrical and optical properties is also studied.

2. Experimental details

Nd-doped pyrite samples were prepared by flash evaporation of mixed FeS_2 and Nd_2O_3 powdered on a glass substrate. Details on this growth procedure can be found elsewhere [14].

The starting material was pyrite powder obtained from natural samples from Logroño (Spain) finely ground until particles of size ranging from 50 to 75 μm were obtained. The composition of this natural pyrite was analysed by x-ray fluorescence as containing 55.2 wt% S and 43 wt% Fe with an impurity level of 530 ppm Ni and 88 ppm Zn. The levels of other impurities detected were below 10 ppm. As a dopant, Nd_2O_3, grade I Johnson–Matthey powder, was added to the pyrite powder to obtain a 10 mol% Nd concentration in the mixture.

Substrates were placed on a holder–heater to maintain the temperature at about 425 K during the deposition process. $FeS_2 + Nd_2O_3$ mixed powder falls from a vibrating dispenser cylinder through a quartz tube onto a tungsten boat heated at 1650 K to produce the instantaneous sublimation of the particles which arrive at the substrate. By this procedure we have obtained films from 0.42 to 0.75 μm thick measured by a Dektak 3030 profilometer. The difference in thickness is due to the different distance of each sample to the evaporation source.

In order to improve the crystalline quality, as well as the stoichiometry of the obtained films, the obtained samples were annealed at different temperatures in the range from 573 to 773 K in a sulphur atmosphere using closed ampoules. This is required to increase the S content in the films which is partially lost during the deposition process [15]. The amount of sulphur introduced was that needed to keep a nominal pressure of 300 Torr in the ampoule for each annealing temperature. The sample thickness did not change after the annealing relative to that of the as-grown samples.

X-ray diffraction (XRD) diagrams of the films were recorded in a Siemens D5000 diffractometer in the usual θ–2θ couple mode with monochromatized Cu Kα ($\lambda = 1.5418$ Å) radiation. Least-squares structure refinements were undertaken with the full-profile, Rietveld type, program DBWS-9006PC, prepared by Sakthiveld and Young [16]. Crystallite size and microstrain distribution was carried out using a Warren–Averback analysis from the Gaussian content and the full widths at half maximum from the refined 2θ peak positions [17]. Details on this microstructural analysis method are reported elsewhere [18].

Resistivity measurements were performed by the four-contact Van der Pauw method [19].

Absorption spectra were recorded in a Hitachi U-3501 spectrophotometer in the range 0.5–3.0 μm. A glass plate identical to the substrate was placed in the reference channel of the spectrophotometer.

Luminescence measurements have been performed by exciting with a cw Ti–sapphire laser tuned in the range 750–870 nm. Measurements have been performed at 15 K using a closed cycle He cryostat. A cooled GaAsIn photomultiplier tube followed by a photon counting gated system and an Si photodiode were used for the detection.

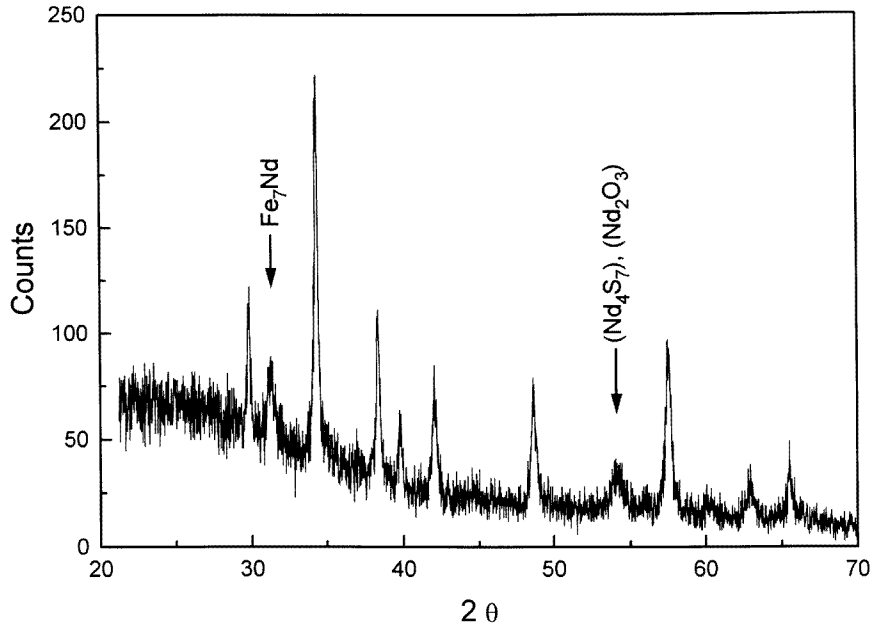

Figure 1. X-ray diffraction spectrum of an Nd:FeS_2 sample obtained by flash evaporation.

3. Results

3.1. Structural properties

Figure 1 shows the x-ray diffraction spectrum of an as-grown sample. The peaks corresponding to pyrite structure are clearly observed (those without arrows on the figure). As expected, some other low-intensity reflections at 30, 38 and 53° of 2θ positions are also observed in the spectrum indicating the presence of Nd in the samples. These peaks can be associated with iron–neodymium alloy (Fe_7Nd), neodymium oxide (Nd_2O_3) and neodymium sulphide (Nd_4S_7) respectively. X-ray spectra of all the samples prepared have been refined and the parameters corresponding to the pyrite lattice have been obtained. Values of some of them are in the following ranges: lattice parameter a, [5.422–5.425 Å]; sulphur positional coordinate u, [0.387–0.397]; sulphur–iron relation S/Fe, [1.71–1.80]. The variation of these parameters among the different samples, prepared in similar conditions, can be related to a different distance of each sample to the evaporation source.

Each one of the samples was annealed at a different temperature in the range 573–773 K for 20 hours in a sulphur atmosphere of 300 Torr. The XRD spectra of the annealed samples showed different characteristics which depend on the annealing temperature when comparing to the as-evaporated samples. Figure 2(a) and (b) shows the spectra corresponding to two samples annealed at 623 and 723 K respectively. As observed, no peaks corresponding to the previously observed Nd compounds (i.e. Fe_7Nd, Nd_2O_3 and Nd_4S_7) were detected in the spectra after the annealing treatments. However, Nd presence in the films has been detected by Rutherford back-scattering (RBS) in all the samples and no Nd diffusion into the glass substrate was observed by this technique (see figure 3, as an example). For annealing temperatures above 720 K, besides the pyrite structure a new Nd phase, different

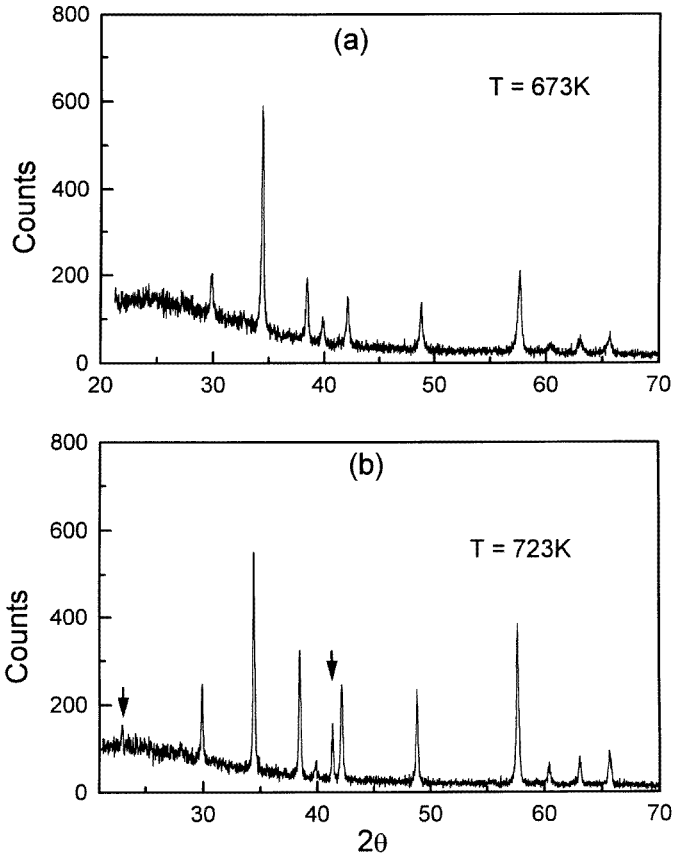

Figure 2. X-ray diffraction spectra for two samples annealed at different temperatures: (a) $T = 673$ K and (b) $T = 723$ K.

to the previously observed ones, appears. The reflections corresponding to this new phase are marked with arrows in figure 2(b). This Nd phase can be associated with the NdS_2 structure (ASTM 26-1278).

Another feature observed in the spectra of the annealed samples is the improvement of the crystalline quality after the thermal treatment. As observed in figure 2 the peaks corresponding to pyrite reflections are more intense and narrower than those obtained for the case of as-grown samples (see figure 1).

The Rietveld refining of the XRD data has been performed, considering only those peaks corresponding to pyrite structure.

From the peak profiles it is possible to obtain more information on the crystal quality of the prepared films. The values of the volume-weighted crystallite size, $\langle D \rangle_v$, along the relevant [*hkl*] directions, as well as the microstrain distribution $\langle \varepsilon^2 \rangle^{1/2}$, have been calculated from the Rietveld refining and a Warren–Averback analysis of the XRD data, respectively. Results are shown in table 1. The obtained value shows an increase in the $\langle D \rangle_v$ value from 230 to 1320 Å as the annealing temperature increases from 570 to 770 K. These values are much higher than those previously obtained for the case of undoped samples, being around twice the value for undoped films [15] for samples annealed at temperatures above

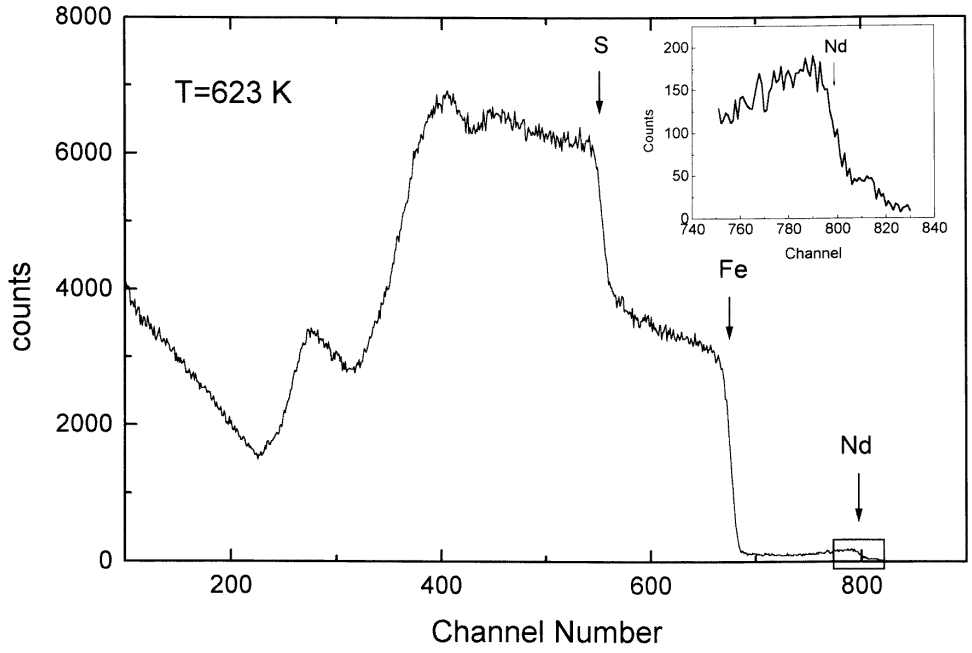

Figure 3. RBS spectrum of an Nd:pyrite film after annealing at 623 K, taken in a 3.1 MeV Van de Graaff accelerator of Instituto Tecnologico e Nuclear in Lisbon. An He^+ beam of 1.6 MeV was used, He^+ beam current being 15 nA.

Table 1. Parameter values for different annealing temperatures for Nd-doped pyrite films: sulphur positional parameter u; S/Fe ratio, crystallite size $\langle D\rangle_v$, microstrain distribution $\langle\varepsilon^2\rangle^{1/2}$, refractive index n, and sample thickness d_0.

T (K)	u	S/Fe	$\langle D\rangle_v$ (Å)	$\langle\varepsilon^2\rangle^{1/2}$	n	d_0 (μm)
573	0.3909(12)	1.72(4)	230			
623	0.3940(15)	1.78(3)	320		3.68	0.72
673	0.3881(6)	1.873(18)	360		3.1	0.75
698	0.3883(14)	1.77(3)	420		3.12	0.73
723	0.3862(6)	1.971(18)	790	4.5×10^{-4}	3.2	0.42
773	0.3932(5)	1.942(17)	1320	1.2×10^{-4}	3.75	0.57

720 K. The microstrain distribution values are lower than for the case of undoped pyrite films grown by the same method. According to this, Nd ions could apparently play some role in improving the crystal quality of the pyrite films.

The data obtained from Rietveld refining calculations for the lattice parameter a, sulphur positional coordinate u, and sulphur–iron relation S/Fe, show variations relative to those obtained for as-grown samples (see table 1).

Figure 4 shows the variation of the lattice parameter a, as a function of the sulphuration temperature, for a series of Nd-doped samples. The lattice parameter decreases for Nd doped samples after the annealing treatment. Moreover, it shows a decreasing behaviour as temperature grows up to 770 K. The same decreasing behaviour is obtained for the case of undoped samples [18], as also observed in figure 4. However, for these samples the lattice parameters are significantly smaller in all cases.

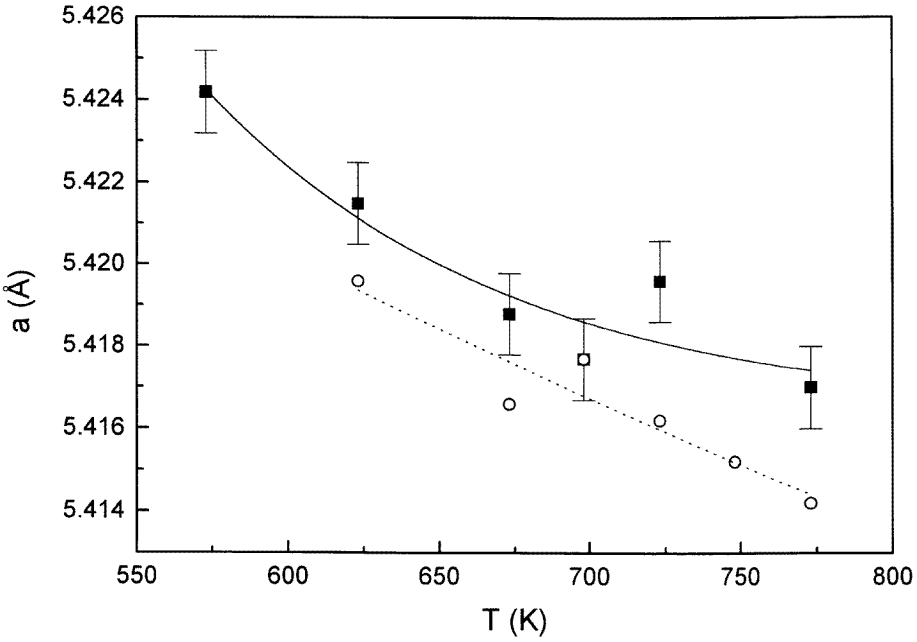

Figure 4. Lattice parameter of the films as a function of the annealing temperature: (■) Nd-doped samples; (○) undoped samples. Lines are guides for eyes.

This decrease of the lattice parameter has been previously explained in the case of undoped films by means of the effect of loss of S atoms, which induce the presence of an increasing number of S vacancies, as the annealing temperature grows. Thus, this effect of S loss should also affect the lattice of Nd-doped pyrite films. However, as it will be shown later, another type of effect has to be considered and taken into account for the decreasing behaviour of the lattice parameter in the case of Nd-doped samples: the fact that Nd-doped pyrite films show a greater value of a relative to undoped samples can be associated with the presence of Nd^{3+} ions in the pyrite films. Since the calculations of a have been performed by taking into account only those peaks corresponding to pyrite structure, avoiding the effects of other crystalline phases, only the Nd dopant ions embedded in the lattice should contribute to that increment of the lattice parameter. It is possible to assume that Nd^{3+} ions should locate in a cationic position, substituting for Fe^{2+} ions into the pyrite lattice. Thus, a distortion of the lattice structure is expected because of the different ionic radii of these two ions and also because of the charge compensation mechanisms appearing when a trivalent ion substitutes for a divalent one in the lattice. However, after annealing treatments at higher temperatures, the values of the lattice parameters of the Nd doped and undoped samples should become similar. As XRD spectra showed, for temperatures above 700 K the majority of the Nd ions form part of the precipitated NdS_2 and the contribution of the remaining Nd ions dissolved into the pyrite structure should be too small to observe changes in the lattice parameter. The variations observed for the high annealing temperature are mainly related to the different stoichiometry between the two types of sample as will be shown later. In the case of undoped samples the S loss is expected to be more important than for Nd-doped samples because a possible charge compensation mechanism needed when Nd^{3+} substitutes for Fe^{2+} in the pyrite structure could be provided by an excess of S ions.

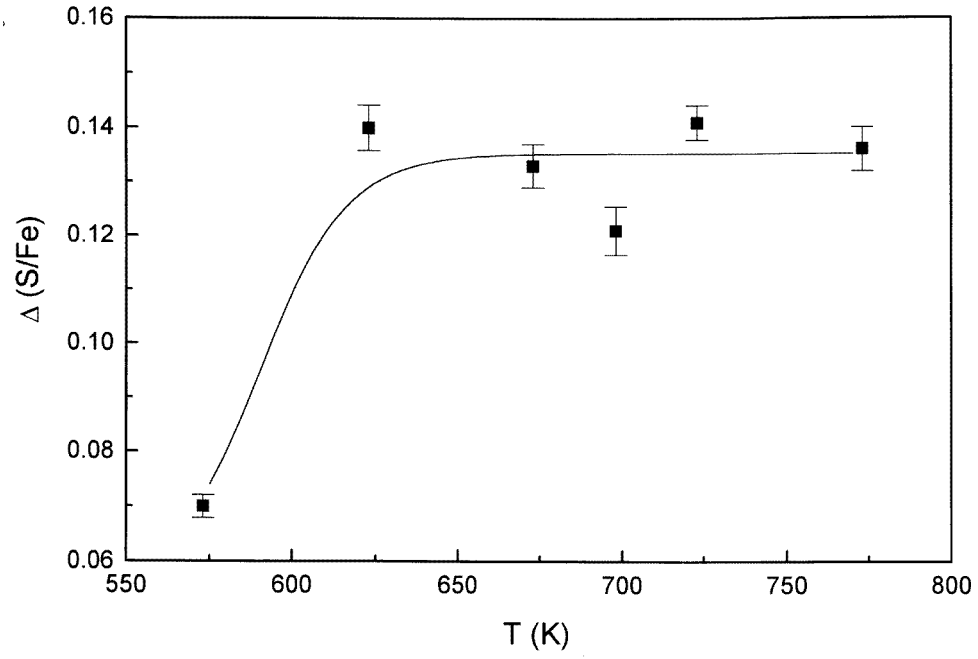

Figure 5. Increment of S/Fe ratio after thermal treatments relative to as-grown samples as a function of the annealing temperature.

The S/Fe relation increases after the annealing in each sample as can be seen in figure 5. There, the increment, $\Delta(S/Fe)$, of that relation after the annealing treatments is represented as a function of the sulphuration temperature. As observed an initial increase of that value from the lowest annealing temperature, 573 K, to the next one, 623 K, occurs, but no significant changes in the quantity $\Delta(S/Fe)$ are observed as annealing temperature is increased to higher values. Thus, the main observed effect is the existence of an annealing temperature range for which an improvement of the stoichiometry is obtained. However, the significance of $\Delta(S/Fe)$ is questionable for the Nd-doped films, since the effect of Nd substituting for Fe ions in the lattice, and the subsequent charge compensation mechanisms, are not taken into account when determining the values of S/Fe.

The relation between the lattice parameter, a, and the S/Fe ratio is shown in figure 6. A diminution of the lattice parameter, a, as the S/Fe ratio increases is observed for Nd-doped films. This behaviour is in the opposite sense to that observed for undoped samples, where the lattice parameter, a, increases with the S/Fe ratio. However, both types of sample approach a similar value of the lattice parameter when the stoichiometry is high. At this point, it should be mentioned that different S/Fe values are obtained for the same annealing temperature for both types of sample.

For undoped samples the dominant effect for the increment of the lattice parameter with the stoichiometry is the increase of S content in the samples, which expands the crystal lattice [18]. However, the different behaviour observed for Nd-doped samples could be mainly related to changes of aggregation stage of Nd ions.

As mentioned, for low annealing temperatures Nd ions could be dissolved into the pyrite lattice producing an increasing of the lattice parameter relative to undoped samples because of the difference in their ionic radius compared to that of Fe ions. This fact

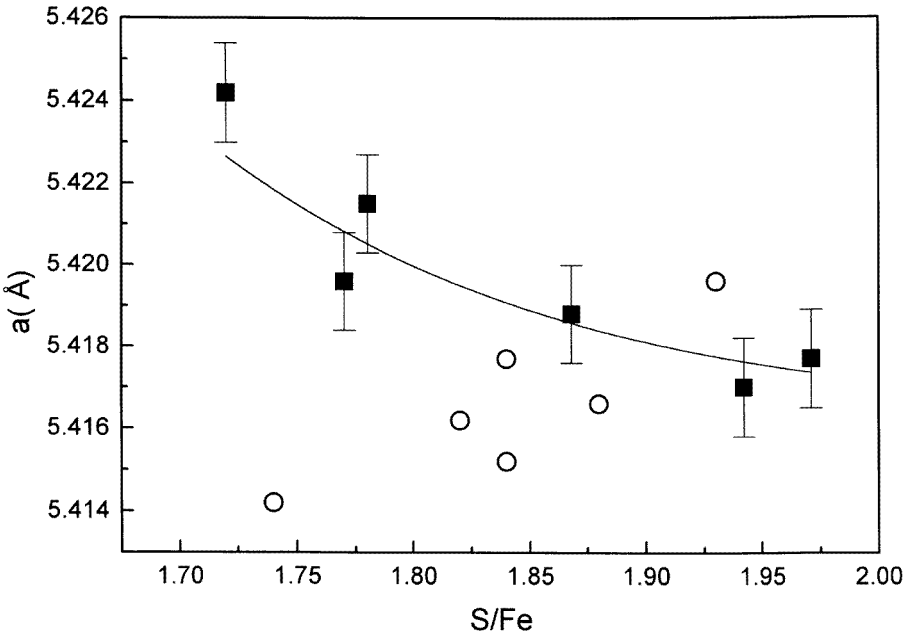

Figure 6. Lattice parameter versus S/Fe ratio for annealed samples: (■) Nd-doped samples; (○) undoped samples.

explains the higher values of *a* observed for doped samples with the lowest S/Fe values. Indeed, the apparent S/Fe value obtained for these samples should not be correlated to the one measured for the undoped samples, because the expected cationic substitution and the subsequent charge compensation mechanisms are not detectable by x-ray diffraction spectra. In fact, those factors should affect the measurement of stoichiometry in the samples.

On the other hand, as the annealing temperature grows, which is directly correlated with S/Fe values in the case of the Nd-doped samples, the NdS_2 crystal phase appears. In that case, the majority of Nd ions are not embedded in the pyrite crystal structure since they form part of a different crystal phase. Thus, the pyrite crystal structure is not strongly distorted (similar lattice parameters are obtained), nor the values of S/Fe ratio, when comparing both doped and undoped samples. As mentioned above, the values of S/Fe for undoped samples represented in figure 6 are not directly correlated to the annealing temperatures.

3.2. Electrical resistivity

Electrical resistivity has been measured in samples before and after the annealing treatments.

Values of the resistivities for as-grown samples are around 2×10^{-3} Ω cm. Hall effect measurements on these samples revealed their p-type nature with a carrier number of about 10^{19} cm^{-3}.

Results relative to Nd-doped samples are shown in figure 7. In this figure the resistivity values for Nd-doped and undoped annealed films as a function of annealing temperature are presented. The obtained values are higher than those of as-evaporated samples. As observed, an increase in the resistivity values with temperature is detected in all types of sample. The resistivity of Nd-doped samples increases from 6×10^{-3} to 1.05 Ω cm as

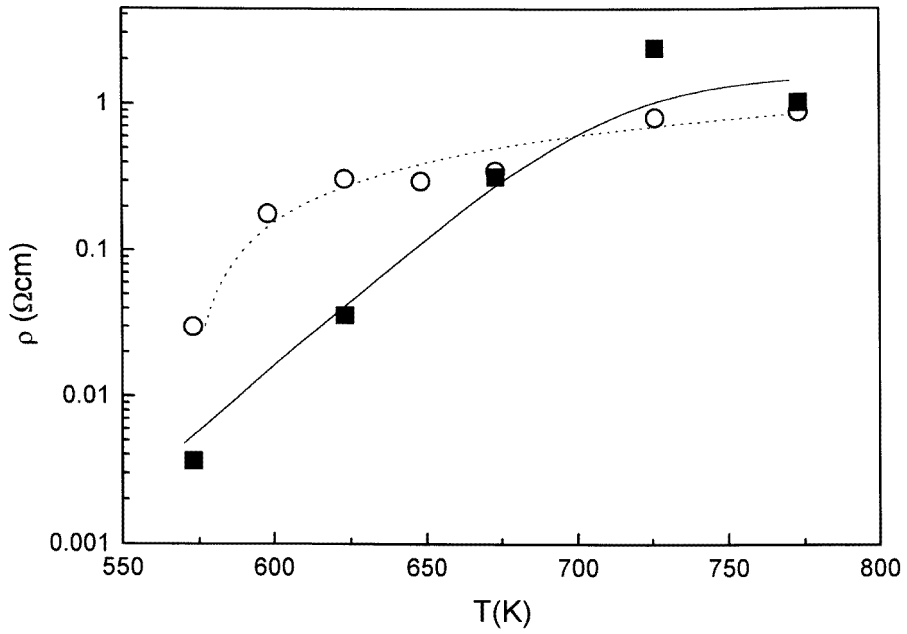

Figure 7. Resistivity values as a function of the annealing temperatures for Nd-doped films (■) and undoped films (○).

the annealing temperature is increased from 570 to 770 K respectively. This behaviour has been previously explained for undoped pyrite films by taking into account the polycrystalline nature of the films and therefore the contribution to the resistivity of both grains and grain boundaries [20, 21]. Data of XRD for pyrite films show that annealing treatments increase the crystallinity of films and this should produce the effect of increasing the resistivity.

As shown in figure 7, the variation of resistivity versus annealing temperature shows two regions: for the low temperature values ($\leqslant$700 K) the resistivity of Nd-doped samples is lower than that of the undoped samples, while for high annealing temperatures ($>$700 K) the resistivity values of the two types of sample seem to approach each other.

This effect can be well explained by considering the differences in the Nd stage of aggregation between these two regions, in the same sense as for the case of the structural properties. The presence of Nd ions dissolved into the pyrite lattice can induce a difference in the resistivity. This fact could probably be due to the charge compensation mechanisms needed when Nd^{3+} is substituting Fe^{2+} ions, which should lead to slightly smaller resistivity values relative to those of undoped films. For the case of higher temperatures, as Nd is forming a segregated phase, similar values of resistivity are obtained indicating that the main contribution is due to the pyrite phase.

3.3. Optical properties

Optical absorption spectra of the films have been recorded at normal incidence in the range 0.5–3 μm. Figure 8 shows the spectrum obtained for a sample annealed at 723 K. This spectrum depicts the absorption edge at about 1 eV and a background modulated by interference fringes for the lower-energy region.

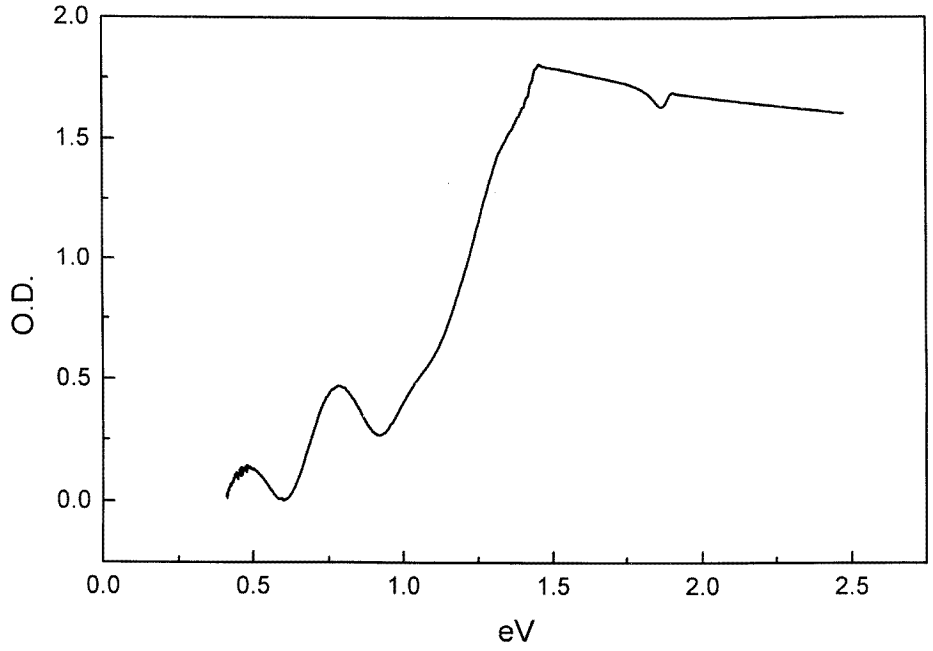

Figure 8. Optical absorption spectrum of an Nd-doped pyrite film annealed at 723 K.

On the obtained spectra the absorption bands corresponding to the intraconfigurational 4f transitions of Nd^{3+} ions were not detectable. The small thickness of the samples makes impossible the observation of these Nd transitions with conventional absorption spectrophotometers. On the other hand, the Nd^{3+} absorption transitions are expected to occur mainly in the visible region where they should be masked by the pyrite absorption edge.

An analysis of the absorption spectra in the range 0.8–3.0 μm can be performed using a non-linear fitting which considers the absorption coefficient as due to three main contributions: an absorption background, α_b, due to the polycrystalline nature of the samples, a linear absorption term and the contribution due to the absorption edge for an indirect transition near to 1 eV [21]. From the fitting, values of the absorption background, α_b, optical energy gap, E, refraction index, n, and sample thickness, d_0, are obtained.

Values of the absorption background diminish as the annealing temperature increases, as observed in figure 9(a). This effect can be related to an increase in the crystallite size which is directly related to the annealing temperature. Thus, the contribution of the boundary grains to the scattering decreases.

Figure 9(b) shows the variation of the optical gap as a function of the annealing temperature. The results are compared to those of undoped samples. The main observed effect is the diminution of the absorption edge energy for the higher temperatures. This fact could be related with an inhomogeneous broadening of the corresponding interband transition, due to the presence of the NdS_2 phase. No clear effect on the absorption spectra could be directly associated with Nd^{3+} ions in the samples.

Refractive index at $E = 1$ eV and thickness values of the films obtained by the fitting are shown in table 1. The refractive index values are similar to those obtained for undoped samples [21].

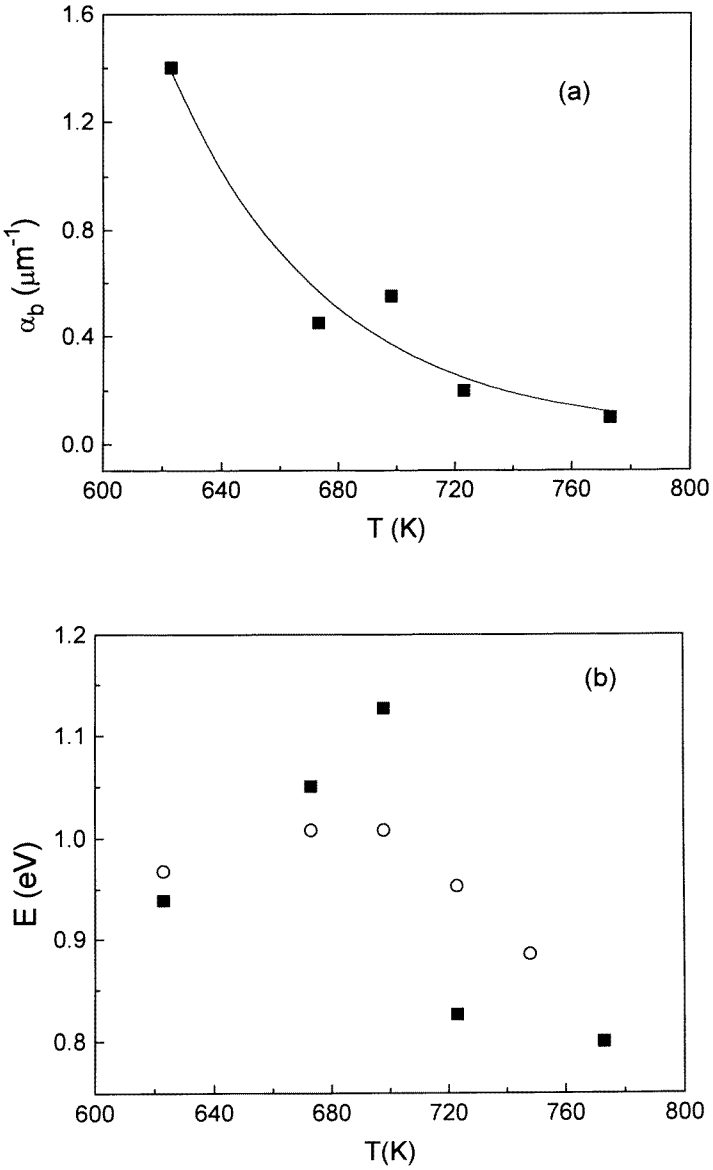

Figure 9. (a) Absorption background α_b as a function of annealing temperatures for Nd-doped pyrite films; (b) energy gap versus annealing temperatures: (■) Nd-doped and (○) undoped films.

The values of sample thickness obtained from the absorption spectra are also shown in table 1. These values were similar to those obtained by direct measurements by profilometry. This fact is in agreement with RBS measurements where no diffusion of pyrite constituents nor Nd ions into the substrates was observed, contrasting to the case of pyrite films obtained by a different method [21].

Fluorescence signals were studied in the emission region (between 860 and 920 nm) where the $^4F_{3/2} \rightarrow {}^4I_{9/2}$ transition of Nd ions is expected. For samples treated at

temperatures above 700 K a small and broad band centred around 887 nm was obtained. The observed band appears to be complex though it did not clearly reveal the typical structure associated with the different Stark transitions involved. This signal was not observed for the case of undoped samples or for samples annealed at lower temperatures.

A more detailed study involving site selective spectroscopy measurements is now under way to determine the nature of the centres responsible for this emission.

4. Conclusion

Neodymium-doped pyrite thin films have been obtained for the first time in this work by flash evaporation of natural pyrite and Nd_2O_3 powder. Thermal annealing improves the crystalline properties and also changes the aggregation stage of neodymium in the samples. For temperatures below 700 K, indirect evidence suggests that most neodymium ions could be dissolved into the pyrite lattice, leading to some modifications of the pyrite crystalline properties, such as a lattice parameter enlargement and a decrease of the electrical resistivity. These parameters display a monotonic variation as the annealing temperature is increased, indicating that the formation of a new phase could be taking place. For annealing temperatures above 700 K diffusion of Nd ions into pyrite lattice is large enough to produce a detectable segregated phase which can be identified as NdS_2 by the XRD spectra. The presence of this new phase in the doped samples leads to values of the studied parameters for the pyrite phase similar to those obtained for undoped samples.

Acknowledgments

The authors wish to thank J García Sole for critical reading of the manuscript. The assistance of A López-Carrizosa and F Moreno is also gratefully acknowledged. The authors thank the Technological and Nuclear Institute of Lisbon where RBS measurements were performed. This work has been done with the support of the Spanish CICYT under contracts PB93-0266 and MAT95-0152.

References

[1] Lallier E, Pocholle J P, Papuchon M, De Micheli M P, Li M J, Qing He, Ostrowsky D B, Grezes-Besset C and Pelletier E 1991 *IEEE J. Quantum Electron.* **QE-27** 618
[2] Chartier I, Ferrand B, Pelenc D, Field S J, Hanna D C, Large A C, Sheperd D P and Tropper A C 1992 *Opt. Lett.* **17** 810
[3] Bausá L E, Lifante G, Daran E and Pernas P L 1996 *Appl. Phys. Lett.* **68** 23
[4] Jones J K, de Sandro J P, Hempstead M, Sheperd D P, Large A C, Tropper A C and Wilkinson J S 1995 *Opt. Lett.* **20** 13 1477
[5] Kaminskii A A 1981 *Laser Crystals* (New York: Springer)
[6] Ennen H, Wagner J, Müller H D and Smith R S 1987 *J. Appl. Phys.* **61** 4877
[7] Klein P B, Moore F G and Dietrich H B 1991 *Appl. Phys. Lett.* **58** 502
[8] Michel J, Benton J L, Ferrante R F, Jacobson D C, Eaglesham D J, Fitzgerald E A, Xie Y H, Poate J M and Kimerling L C 1991 *J. Appl. Phys.* **70** 2672
[9] Hogg R A, Takahei K and Taguchi A 1996 *J. Appl. Phys.* **79** 8682
[10] Wagner J, Ennen H and Müller H D 1986 *J. Appl. Phys.* **59** 1202
[11] Peale R E, Summers P L, Weidner H, Chai B H T and Morrison C A 1995 *J. Appl. Phys.* **77** 270
[12] Ferrer I J, Caballero F, de las Heras C and Sanchez C 1993 *Solid State Commun.* **70** 588
[13] Miura N, Sasaki T, Matsumoto H and Nakano R 1992 *Japan. J. Appl. Phys.* **31** 51
[14] de las Heras C and Sánchez C 1991 *Thin Solid Films* **199** 259
[15] de las Heras C, Ferrer Y J and Sánchez C 1993 *J. Appl. Phys.* **74** 4551

[16] Sakthiveld A and Young R A 1991 *User Guide to Programs DBWS-9006 and DBWS-9006PC for Rieltveld Analysis of x-Ray and Neutron Powder Diffraction Patterns* (Atlanta, GA: Georgia Institute of Technology)
[17] Klug H P and Alexander L E 1994 *X-Ray Diffraction Procedures for Polycrystalline and Amorphous Materials* (New York: Wiley–Interscience)
[18] de las Heras C, Martín de Vidales J L, Ferrer I J and Sanchez C 1996 *J. Mater. Res.* **11** 211
[19] Van der Pauw 1958 *Philips Res. Rep.* **13** 1
[20] Volger J 1950 *Phys. Rev.* **79** 1023
Petriz R L 1956 *Phys. Rev.* **104** 1508
[21] de las Heras C and Lifante G 1997 *J. Appl. Phys.* accepted for publication